

Sensitive Electrochemical Determination of Morphine Using Gold Nanoparticles–Ferrocene Modified Carbon Paste Electrode

Nada F. Atta^{1,*}, Ahmed Galal¹, Anwar A. Wassel², Asmaa H. Ibrahim²

¹ Department of Chemistry, Faculty of Science, Cairo University, 12613 Giza, Egypt,

² National Organization for Drug Control and Research (NODCAR), Giza, Egypt

*E-mail: nada_fahl@yahoo.com

Received: 28 August 2012 / Accepted: 8 October 2012 / Published: 1 November 2012

An effective electrochemical sensor based on carbon paste (CP) electrode with ferrocene /gold nanoparticles GNFMCPPE, is introduced for selective determination of morphine (MO) in presence of interference compounds as ascorbic acid (AA) and uric acid (UA). Furthermore, the modified electrode is used for simultaneous determination in presence of dopamine (DA) or l-norepinephrine (NEP) in 0.04 mol L⁻¹ universal buffer solution (B-R) (pH 7.4), a well defined oxidation peaks with high current response and good potential peak separation is obtained compared to the unmodified electrode. The electrochemistry of MO is investigated by cyclic voltammetry (CV), differential pulse voltammetry (DPV) and electrochemical impedance measurements (EIS). The morphine concentration could be measured in the concentration range of 1.0×10⁻⁶ to 18.0×10⁻⁴ mol L⁻¹ with a detection limit of 3.507 x 10⁻⁹ mol L⁻¹ and a correlation coefficient of 0.9994. The sensor has also been successfully applied to the determination of morphine spiked into diluted urine samples with a low detection limit and satisfied recovery. The good results indicate that GNFMCPPE holds great promise in practical application.

Keywords: Sensor; Carbon paste electrode; Ferrocene carboxylic acid; Gold nanoparticles; Morphine; Urine samples.

1. INTRODUCTION

Morphine was the first active principle purified from a plant source and is one of at least 50 alkaloids of several different types present in opium. As a major component in opium, morphine is often used to relieve severe pain in patients, especially those undergoing a surgical procedure. It is recommended by the World Health Organization (WHO) for the relief of moderate cancer-related pain [1]. However, it is toxic in excess and when abused.

Different methods have been used for the determination of morphine in plasma, urine, and opium samples, such as gas chromatography (GC) [2], liquid chromatography (LC) [3], high performance liquid chromatography (HPLC) [4], ultraviolet (UV) spectroscopy [5], immunoassay, such as surface plasmon resonance (SPR) based immunosensors [6,7], radioimmunoassays (RIA) [8], molecular imprinting technique [9,10], amperometric methods [11,12], chemiluminescence [13] and electrochemical methods [14–18] are also reported for morphine detection. Among them, electrochemical methods have also received much interest due to their higher selectivity, lower cost and faster operation than other methods. Bare electrodes as glassy carbon electrode [19] platinum and graphite electrode [20] are used in detection of morphine. Recently, various modified electrodes have been reported for the electrochemical detection of MO as cobalt hexacyanoferrate modified glassy carbon electrode (GCE) [14], Prussian blue-modified indium tin oxide (ITO) electrode [15], molecularly imprinted polymer films to fabricate a microfluidic system for amperometric detection of MO [16], chemically modified-palladized aluminum electrode [21], Au microelectrode [22,23] in a flow injection system and also multiwalled carbon nanotubes modified preheated glassy carbon electrode has also been used for the morphine detection [24], PEDOT modified Pt-electrode [18] and gold nanoparticles modified carbon paste electrode [25].

Morphine specifically blocks nociceptive stimulation during surgery. The mechanism of action of morphine may have its etiology in concurrent modulation of more than one neurotransmitter. Moreover, in invertebrates, DA acts as the major molecule used in neural systems. In vertebrates, NEP emerges as the major end of the catecholamines. The simultaneous determination of MO with these compounds was studied [18, 25].

Electrodeposition of gold nanoparticles onto the surface of the CP electrode was another strategy to enhance the sensitivity of the immunosensor with large surface area, good biocompatibility, high conductivity and electrocatalysis characteristics, has been used to improve the detection limits in electrochemical studies [26-28]. They are also suitable for many surface immobilization mechanisms and can act as tiny conduction center and can facilitate the transfer of electrons. The modification of surfaces with ferrocene moieties proved to be effective as it adds a faradic component to the process of charge transfer. So, it increases the rate of the charge transfer at the surface-electrolyte interface. Several research groups described the electrochemical behavior and applications of Ferrocene-modified polymer electrode [29-35]. Glassy carbon electrode used for evaluation of ferrocene carboxylic acid confined on surfactant-clay [36]. Other surfaces as CP-electrode modified with ferrocene carboxylic acid and TiO₂ nanoparticles in determination of captopril [37], glutathione and tryptophan [38] and CP-electrode modified with multi-walled carbon nanotubes and ferrocene for sensitive determination of cysteamine and folic acid [39].

For the first time we introduce highly sensitive electrochemical biosensor based on gold nanoparticles/Ferrocene modified carbon paste electrode, to be used for the determination of morphine in presence of interference compounds. The electrochemical behaviors of the drug at our modified electrode will be investigated using CV and differential pulse voltammetry (DPV) techniques. The application of the proposed sensor for simultaneous determination of MO with DA or with 1- NEP will be shown. Moreover the validity of using this method in the determination of MO in spiked urine samples without sample pretreatment will be demonstrated as real sample applications.

2. EXPERIMENTAL

2.1. Materials and reagents

Morphine sulphate, ascorbic acid (AA), uric acid (UA), dopamine (DA), l-norepinephrine (NEP), ferrocene carboxylic acid (FCA), tetrabutylammonium hexafluoro-phosphate (TBAHFP), HPIC grade acetonitrile (AcN), potassium ferrocyanide $K_4 Fe(CN)_6$ and potassium chloride KCl were purchased from Aldrich and were used as received without further purification. Britton–Robinson (B–R) ($4.0 \times 10^{-2} \text{ mol L}^{-1}$) buffer solution of pH 2–9 ($CH_3COOH + H_3BO_3 + H_3PO_4$), was used as the supporting electrolyte. The pH was adjusted using 0.2 M NaOH. All solutions were prepared from analytical grade chemicals and sterilized Milli-Q deionized water.

2.1.1. Construction of gold nanoparticles / ferrocene modified CP-electrode (GNFMCPE)

CP-electrode with a diameter 3 mm was fabricated as described elsewhere [40] then electrodeposition of ferrocene from homogeneous 0.01 mol L^{-1} ferrocenium solution (0.01 mol L^{-1} FCA, 0.01 mol L^{-1} TBAHFP in AcN) was done by applying 75 repeated cycles in a potential range (-0.2V:1.2V) versus Ag/AgCl then the electrode was washed and immersed in 6 mmol L^{-1} hydrogen-tetrachloroaurate $HAuCl_4$ solution containing 0.1 mol L^{-1} KNO_3 (prepared in doubly distilled water, and deaerated by bubbling with nitrogen). A constant potential of $-0.4V$ was applied for 4 min. Then, the modified electrode (GNFMCPE) was washed with doubly distilled water and dried carefully by a paper without touching the surface and then left to dry in air for 10 min. before being used. The effect of changing the number of repeated cycling (10, 25, 50, 75 and 100 cycles) of electrodeposition of ferrocene on modified electrode was studied $1.0 \times 10^{-3} \text{ mol L}^{-1}$ MO in B-R buffer pH 7.4 at scan rate 100 mVs^{-1} (Fig. (1)) and we found that 75cycles give a sharp peak with highest current than the other cases.

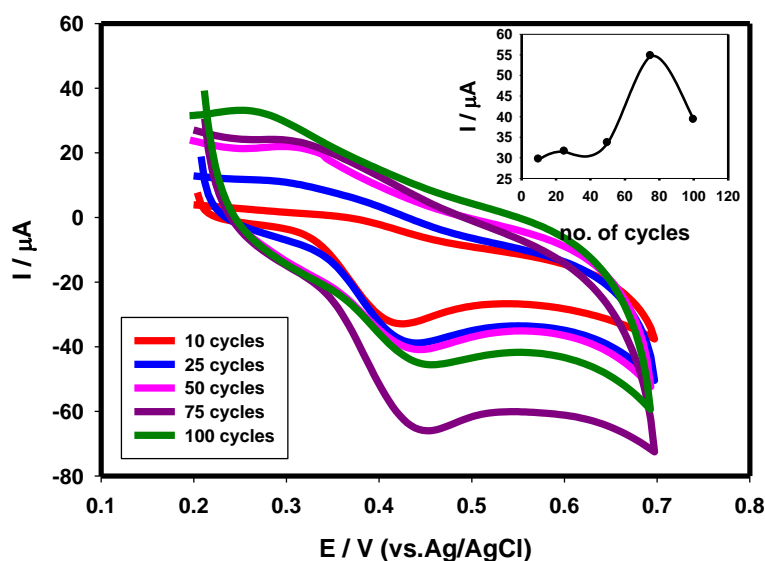


Figure 1. Effect of no. of repeated cycles (10, 25, 50, 75 and 100 cycles) of electrodeposition of ferrocene on CPE after(electrodeposition of Au) in $1.0 \times 10^{-3} \text{ mol L}^{-1}$ MO in B-R buffer pH 7.4 at scan rate 100 mVs^{-1} .

2.2. Instrumental and experimental set-up

2.2.1. Electrochemical measurements

All voltammetric measurements were performed using a personal computer-controlled AEW2 electrochemistry work station and data were analyzed with EC_{prog3} electrochemistry software, manufactured by SYCOPEL SCIENTIFIC LIMITED (Tyne & Wear, UK). The one compartment cell with the three electrodes was connected to the electrochemical workstation through a C₃-stand from BAS (USA). A platinum wire from BAS (USA) was employed as auxiliary electrode. All the cell potentials were measured with respect to Ag/AgCl (3 mol L⁻¹ NaCl) reference electrode from BAS (USA). One compartment glass cell (15 ml) fitted with gas bubbler was used for electrochemical measurements. Solutions were degassed using pure nitrogen prior and throughout the electrochemical measurements. A JENWAY 3510 pH meter (England) with glass combination electrode was used for pH measurements. Scanning electron microscopy (SEM) measurements were carried out using a JSM-6700F scanning electron microscope (Japan Electro Company). All the electrochemical experiments were performed at an ambient temperature of 25±2°C.

2.2.2. Impedance spectroscopy measurements

Electrochemical impedance spectroscopy was performed using a Gamry-750 system and a lock-in-amplifier that are connected to a personal computer. The data analysis software was provided with the instrument and applied non-linear least square fitting with Levenberg-Marquardt algorithm. All impedance experiments were recorded between 0.1 Hz and 100 kHz with an excitation signal of 10 mV amplitude. These parameters were applied for 5.0 x 10⁻³ M K₄[Fe(CN)₆] dissolved in 0.1M KCl on CP-electrode, gold nanoparticles modified CPE (AuNpCPE) and GNFMCPPE at potential values 315, 300 and 280 mV respectively.

2.3. Analysis of urine

Successive additions of 1mmol/L MO provided by the National Organization for Drug Control and Research of Egypt were added to 5 ml of diluted urine in B-R buffer (pH 7.4).

3. RESULTS AND DISCUSSION

3.1. Morphologies of the different electrodes

The response of an electrochemical sensor is related to its physical morphology. The SEM of CP-electrode and GNFMCPPE were shown in Fig 2. Significant differences in the surface structure of CP-electrode and GNFMCPPE are observed. The surface of the CP-electrode was predominated by isolated and irregularly shaped graphite flakes and separated layers were noticed (Fig 2A). The SEM image of GNFMCPPE (Fig 2B) shows that multilayer nanoparticles with an irregular distribution and interstices among the nanoparticles were observed in SEM image of the GNFMCPPE exhibiting large surface area.

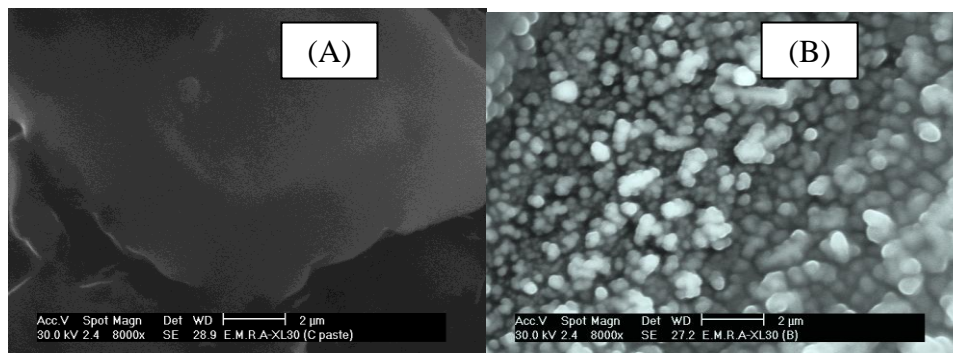


Figure 2. Scanning electron microscope of different electrodes: A) CP-electrode and B) GNFMCPPE.

3.2. Electrochemistry of MO at GNFMCPPE

The voltammetric behavior of MO was examined using cyclic voltammetry. Fig 3 shows typical cyclic voltammograms of $1.0 \times 10^{-3} \text{ mol L}^{-1}$ of morphine (MO) in B-R buffer pH 2 (A) and 7.4 (B), at scan rate 100 mVs^{-1} recorded at different working electrodes (i.e. a bare CP (solid line), AuNpCPE (dotted line) and GNFMCPPE (dashed line) electrodes, respectively). In case of pH 2, at bare CP-electrode, the oxidation peak was observed at 781.96 mV with current response $40.88 \mu\text{A}$, whereas at AuNpCP, the current response increases to $59.80 \mu\text{A}$ due to the improvements in the reversibility of the electron transfer process and a larger real surface area of the modified electrode. Furthermore the electrodeposition of Au nanoparticles on ferrocene modified CP-electrode resulted in an observable increase in the peak current to $107.96 \mu\text{A}$, which indicates an improvement in the electrode kinetics and a decrease in the potential of oxidation substantially to 731.81 mV. In case of pH 7.4, at bare CP-electrode, the oxidation peak was observed at 517.40 mV with current response $16.81 \mu\text{A}$, whereas at AuNpCP, the current response increases to $29.03 \mu\text{A}$ due to the improvements in the reversibility of the electron transfer process and a larger real surface area of the modified electrode. Furthermore the electrodeposition of Au nanoparticles on ferrocene modified CP-electrode resulted in an observable increase in the peak current to $54.7 \mu\text{A}$, which indicates an improvement in the electrode kinetics and a decrease in the potential of oxidation substantially to 454.98 mV (i.e. thermodynamically feasible reaction). The aforementioned results confirm the synergism of ferrocene carboxylic acid and gold nanoparticles where the incorporation of the ferrocenium to the paste increases the electronic conduction of the paste and consequently increases the rate of the charge transfer at the paste-electrolyte interface. So it added a faradaic component to the process of charge transfer [41, 42]. The Au nanoparticles beside they increase the surface area, they act as a promoter to enhance the electrochemical reaction. The oxidation peak is attributed to the oxidation reaction of the phenolic group (-OH) at the 3-position which involves one-electron transfer and is responsible for the major peak. The oxidation of the phenolic group leads to the formation of pseudomorphine (PM) as the main product. Since the structure of pseudomorphine possesses two phenolic groups it makes its further oxidation possible. However, as shown in Figure 3, the oxidation occurs at the same potential as morphine. Therefore the oxidation peak is ascribed to oxidation of the phenolic groups in morphine and pseudomorphine according to:

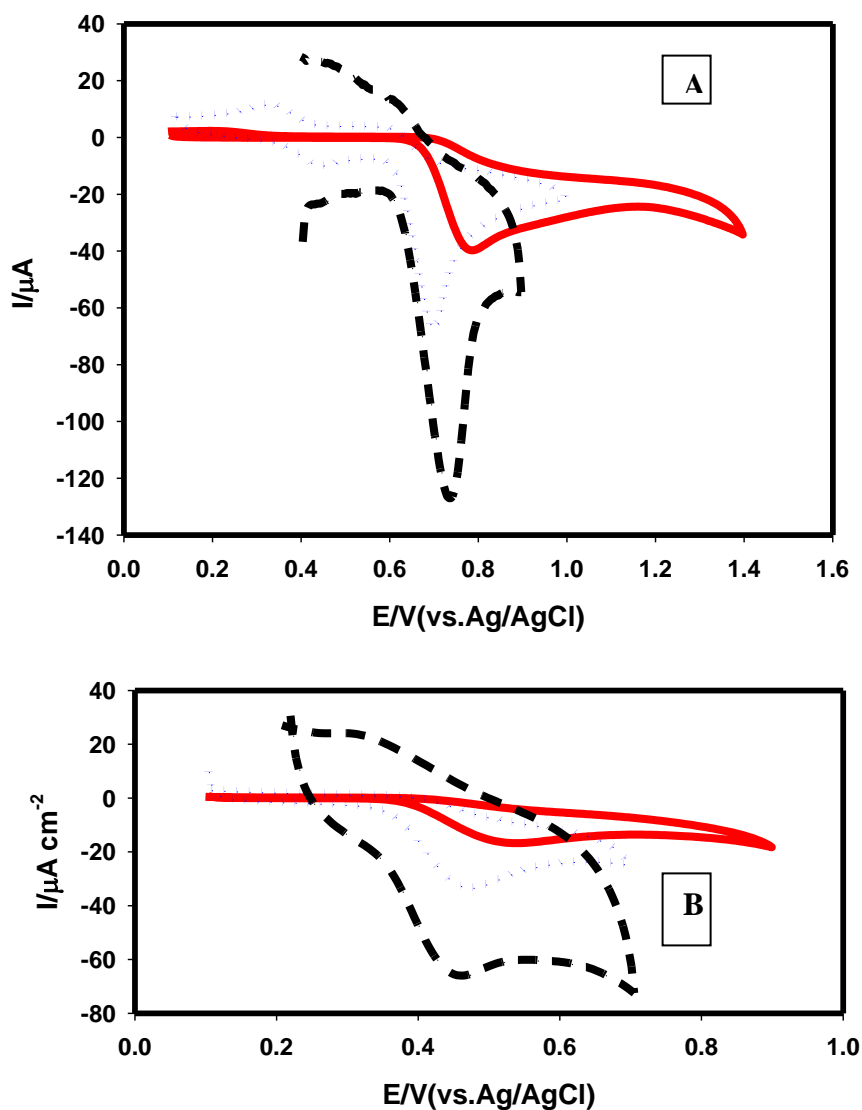
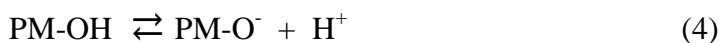
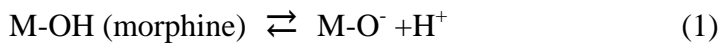


Figure 3. A) Cyclic voltammograms of $1.0 \times 10^{-3} \text{ mol L}^{-1}$ MO in B-R buffer pH 2 at scan rate 100 mVs^{-1} recorded at three different working electrodes 1) bare CPE (—), 2) AuNpCPE (.....) and 2) GNFM CPE (----). B) Cyclic voltammograms of $1.0 \times 10^{-3} \text{ mol L}^{-1}$ MO in B-R buffer pH 7.4 at scan rate 100 mVs^{-1} recorded at three different working electrodes 1) bare CPE (—), 2) AuNpCPE (.....) and 2) GNFM CPE (----).

3.3. Effect of operational parameters

3.3.1. Effect of solution pH

Figure 4A shows the cyclic voltammograms of the oxidation of MO at different pH ranges (2 → 9) using Britton–Robinson buffer. The peak current values were obtained by subtracting the background current of the GNFMCPPE obtained in the pure supporting electrolyte solution from the anodic peak current obtained for MO oxidation.

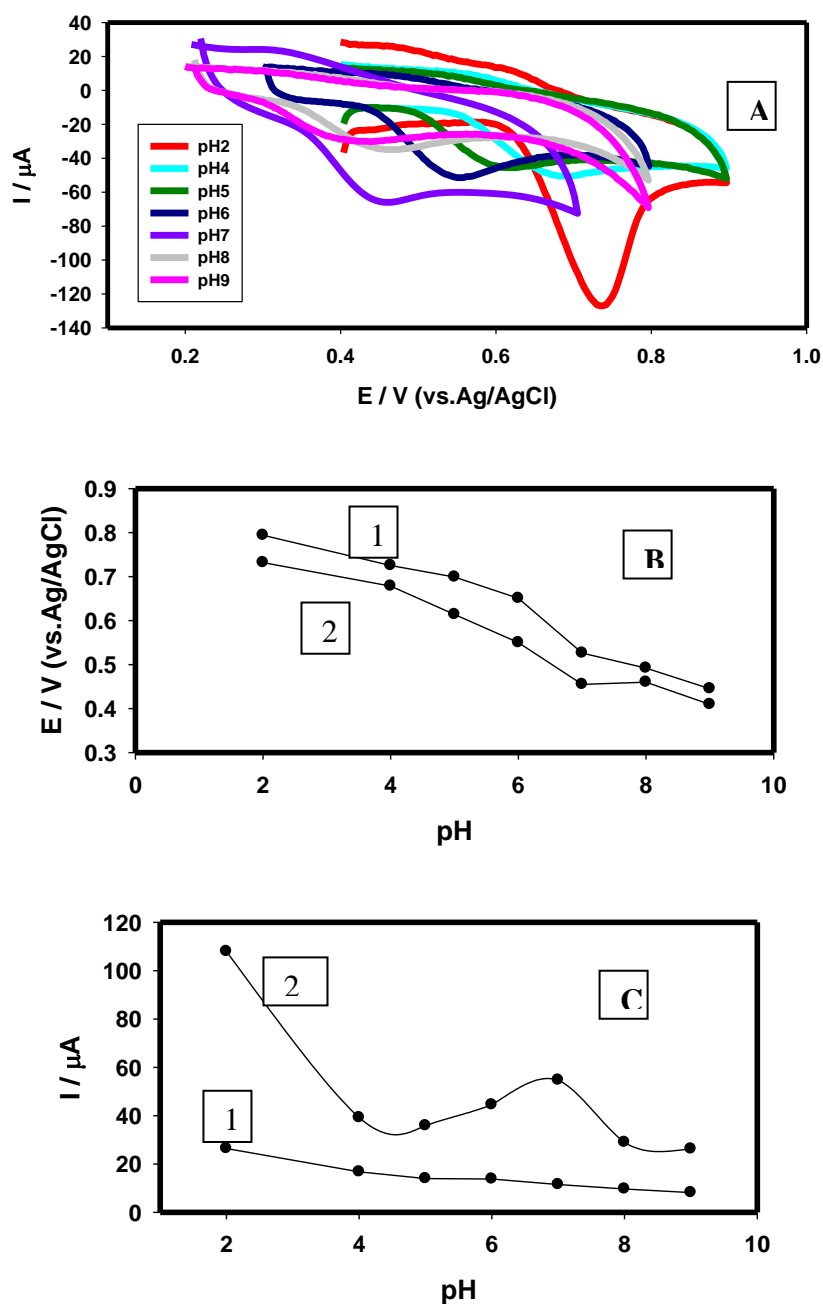


Figure 4. A) cyclic voltammogram of the effect of solution pH on the electrocatalytic oxidation of $1.0 \times 10^{-3} \text{ mol L}^{-1}$ MO at GNFMCPPE using Britton–Robinson buffers within the pH range of 2–9. B) Comparison between the anodic peak potentials at different pH values of 1) bare CPE and 2) GNFMCPPE. C) Comparison between the anodic peak currents at different pH values of 1) bare CPE and 2) GNFMCPPE.

A comparison between the anodic peak potential at different pH values of bare CPE and GNFMCPe (fig 4B) shows that the pH of the solution has a significant influence on the peak potential of the catalytic oxidation of MO, i.e. the anodic peak potentials shifted negatively with the increase of the solution pH, in both cases indicating that the electrocatalytic oxidation at the GNFMCPe is a pH-dependent reaction and that protons have taken part in their electrode reaction processes.

Also, the peak potential for MO oxidation varies linearly with pH (over the pH range from 2 to 9). The relationship between the anodic peak potential and the solution pH value (over the pH range from 2 to 9) could be fit to the linear regression equation of $E_{pa} \text{ (V)} = 0.859 - 0.051 \text{ pH}$, with a correlation coefficient of $r = 0.994$. The slope was found to be -51 mV/pH units over the pH range from 2 to 9, which is close to the theoretical value of -59 mV . This indicated that the number of protons and transferred electrons involved in the oxidation mechanism is equal [43]. As the MO oxidation is one-electron process, the number of protons involved was also predicted to be one indicating an e^-/H^+ process. Although the highest oxidation peak current was obtained at pH 2, other factors will be studied at pH 7.4 (i.e. pH medium of the human body).

Also the comparison between the anodic peak current at different pH values of bare CPE (1) and GNFMCPe (2) (fig 4C) shows that by using GNFMCPe, the oxidation of MO gave high anodic current responses at all pH values with noticeable highest current response at pH value 2 and 7. Knowing that the pKa of morphine value is 8.08 [44], therefore, the positive charge on MO can be attracted by the gold nanoparticles negative charge, which indicates the effect of gold nanoparticles on the catalytic oxidation processes beside the enhancement effect of electron charge transfer by the ferrocene.

3.3.2. Stability of the response of the modified electrode

In order to investigate the response stability of GNFMCPe, the CV for $1.0 \times 10^{-3} \text{ mol L}^{-1}$ MO in B-R buffer (pH7.4) solution were recorded every five minutes and it stands for fifty runs (Fig. 5).

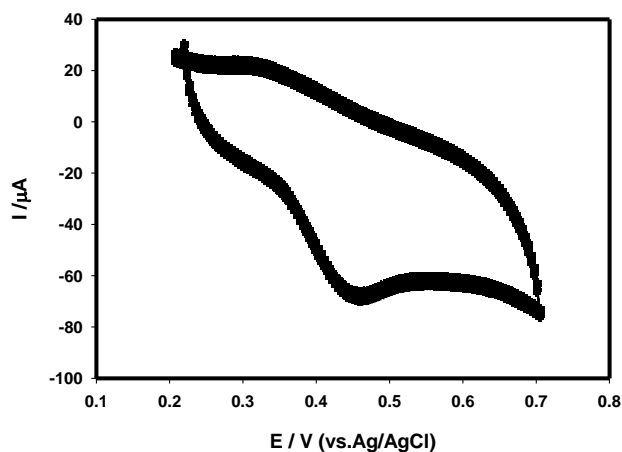


Figure 5. Cyclic voltammograms (CV) for $1.0 \times 10^{-3} \text{ mol L}^{-1}$ MO at the GNFMCPe in 0.04 M B-R buffer (pH 7.4) solution recorded every five minutes for fifty runs.

It was found that the anodic and cathodic peak currents remained practically the same. Repetitive measurements indicated that this electrode has good reproducibility and does not undergo surface fouling during the voltammetric measurements.

3.3.3. Influence of the scan rate

The effect of different scan rates (v ranging from 10 to 250 mVs^{-1}) on the oxidation current response of MO ($1.0 \times 10^{-3} \text{ mol L}^{-1}$) at GNFMCPPE in B-R buffer (pH 7.4) was studied and a plot of i_{pa} versus $v^{1/2}$ gave a straight line relationship. This revealed that the linearity of the relationship was realized up to a scan rate of 250 mVs^{-1} . This indicated that the charge transfer was under diffusion control. Typical CV curves of MO at different scan rates were shown in Fig 6. The peak potential also increased with increasing the scan rate. A good linear relationship was found for the oxidation peak currents at different scan rates (Fig 6 inset). The oxidation peak currents increased linearly with the linear regression equations as $i_{\text{pa}} (10^{-6} \text{ A}) = 5.353 v^{1/2} (\text{V s}^{-1})^{1/2} - 6.016$ ($n=7$, $\gamma = 0.9983$), suggesting that the reaction is diffusion-controlled electrode reaction.

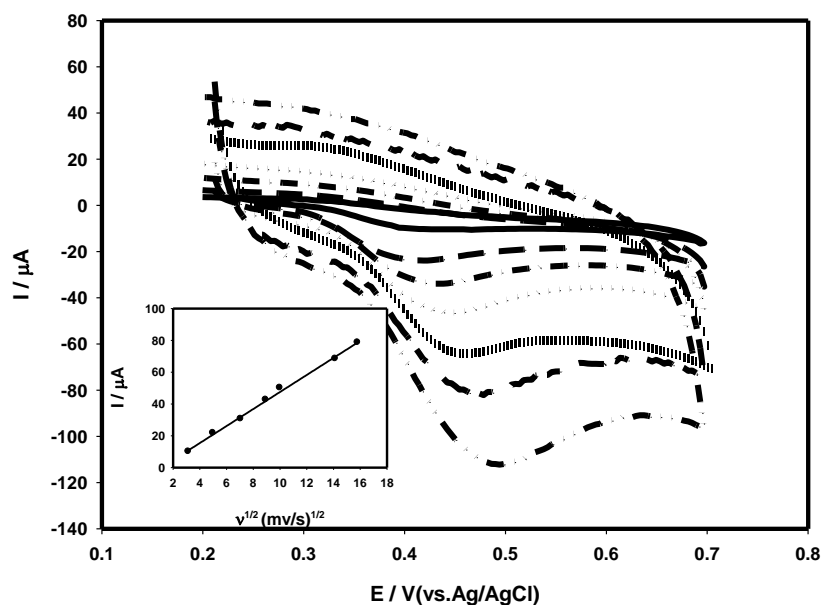


Figure 6. Cyclic voltammograms of $1.0 \times 10^{-3} \text{ mol L}^{-1}$ MO at GNFMCPPE in 0.04 M B-R buffer pH 7.4 at: 10, 25, 50, 80, 100, 200 and 250 mV s^{-1} . The inset: plot of the anodic peak current values versus square root of scan rate.

3.3.4. Diffusion coefficients of MO

The dependence of the anodic peak current density on the scan rate has been used for the estimation of the “apparent” diffusion coefficient, D_{app} , for the compounds studied. D_{app} values were calculated from Randles Sevcik equation [31]

$$i_{pa} = (2.69 \times 10^{-5}) n^{3/2} A C_0 D_0^{1/2} v^{1/2}$$

Where the constant has units (i.e. $2.687 \times 10^5 \text{ C mol}^{-1} \text{ V}^{-1/2}$).

In these equations: i_{pa} is the peak current density (mA cm^{-2}), n is the number of electrons appearing in half-reaction for the redox couple, v is the rate at which the potential is swept (V s^{-1}), F is Faraday's constant (96485 C mol^{-1}), C_0 is the analyte concentration ($1 \times 10^{-6} \text{ mol cm}^{-3}$), A is the electrode area (0.0706 cm^2), and D is the electroactive species diffusion coefficient ($\text{cm}^2 \text{ s}^{-1}$). Apparent surface area used in the calculations did not take into account the surface roughness.

The apparent diffusion coefficients, D_{app} , of MO on GNMCPPE in B-R buffer (pH 7.4) were calculated from cyclic voltammetry (CV) experiments and was found to be $9.94 \times 10^{-6} \text{ cm}^2 \text{ s}^{-1}$ this result was compared to that in case of bare CP-electrode which is $2.96 \times 10^{-6} \text{ cm}^2 \text{ s}^{-1}$. This indicated the quick mass transfer of the analyte molecules towards electrode surface from bulk solutions and/or fast electron transfer process of electrochemical oxidation of the analyte molecule at the interface of the electrode surface and the solution interface [45, 46]. Furthermore, it also showed that the redox reaction of the analyte species took place at the surface of the electrode under the control of the diffusion of the molecules from solution to the electrode surface. The calculated D_{app} values for MO at bare CP-electrode and GNFMCPE show that Au nanoparticles on electrodeposited ferrocene improve the electron transfer kinetics at the electrode/solution interface.

3.4. Action of MO on biological compounds

3.4.1. Morphine, ascorbic acid and uric acid.

Acute and chronic morphine administrations increase dopamine (DA), turnover [47] and release [48] in terminal fields of dopaminergic neurons. Increased dopaminergic activity in the limbic area and in the striatum is paralleled by increased locomotor activity and stereotyped behavior [49]. The dopaminergic system is also involved in the reinforcing effects of abused drugs [50]. Experimental evidence suggests that ascorbic (AA) may modulate central dopaminergic transmission [51] as well as behavior [52]. AA is not synthesized in the brain, and then diffuses at the blood-brain barrier site. AA is a very active component of the neuronal antioxidant pool, since it is rapidly oxidized by reactive oxygen species (ROS) [53]. AA is the main scavenger of ROS generated from catecholamine oxidation in vivo [54].

It is well known that large doses of AA have been reported to suppress withdrawal symptoms in opiate addicts and to prevent the development of tolerance and physical dependence on MO. Moreover, MO, increases UA levels and AA oxidation. Therefore, the electrochemical behavior of MO in the presence of high concentration of AA and UA is very crucial from the clinical point of view. The GNFMCPE was used for voltammetric detection of MO in the presence of AA and UA (mixture (I): 5.0 mM AA, 1.0 mM UA and 0.5 mM MO) in B-R buffer pH 7.4, the applied scan rate was 10 mV/s using differential pulse mode. Fig 7-curve AI shows the differential pulse voltammograms obtained with the bare CP-electrode (solid line) and GNFMCPE (dashed line) in $0.5 \times 10^{-3} \text{ mol L}^{-1}$ MO. The anodic peak current increased from 5.87 μA in case of bare CP-electrode to 14.34 μA in case

of GNFMCPPE, at nearly the same oxidation potential. The determination of 5.0×10^{-3} mol L⁻¹ AA on bare CP-electrode (solid line) gives a peak current at 30.03 μ A which disappears using GNFMCPPE(dashed line) (curve AII). Curve AIII shows that the anodic peak current of 1.0×10^{-3} mol L⁻¹ UA decreased from 13.19 μ A in case of bare CP-electrode (solid line) to 6.76 μ A using GNFMCPPE (dashed line). Curve B shows the voltammograms of mixture (I), under the same optimum experimental conditions. As can be noticed in case of bare CP-electrode (solid line) only broad peak for UA,AA and MO has been obtained, while in case of GNFMCPPE (dashed line) one sharp peak with relatively higher peak current for MO at 328.53 mv and another broad peak for uric acid were observed as illustrated in Fig 7B.

The results of this study show that it is possible to determine MO selectively in presence of high concentration of AA and UA by using the proposed modified electrode.

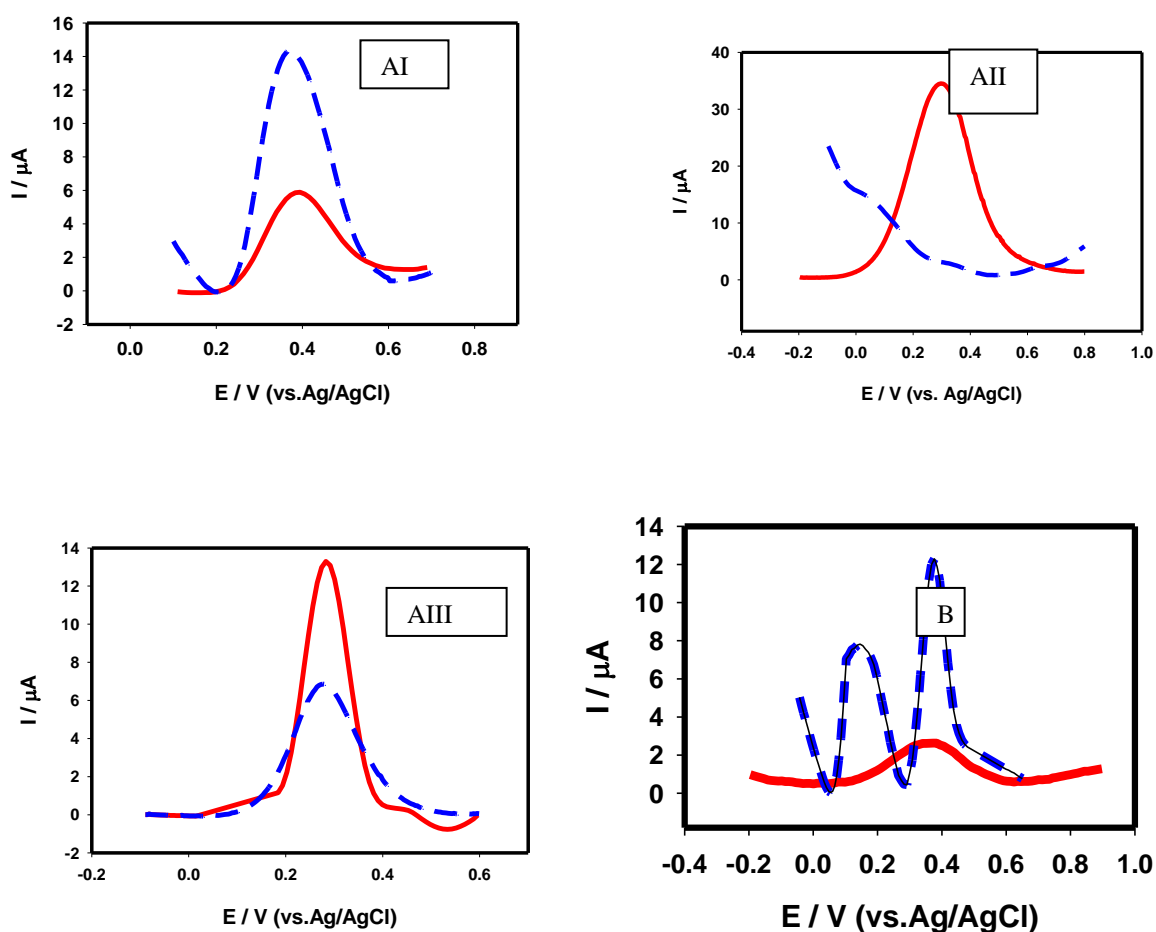


Figure 7. A) The differential pulse voltammograms obtained with the bare CP-electrode (solid line) and GNFMCPPE (dashed line) of I) 0.5 mM MO, II) 5 mM AA and III) 1mM UA, in 0.04 M B-R buffer pH 7.4, scan rate 10 mV/s. B) The differential pulse voltammograms obtained at bare CP-electrode (solid line) and GNFMCPPE (dashed line) for a mixture of 0.5 mM MO + 5 mM AA + 1mM UA in 0.04 M B-R buffer pH 7.4, scan rate 10 mV/s.

3.4.2. Morphine and neurotransmitters

The increase of plasma catecholamines that occurs during surgery can be reduced by administration of morphine. This is due to the fact that morphine specifically blocks nociceptive stimulation during surgery. The mechanism of action of morphine may have its etiology in concurrent modulation of more than one neurotransmitter. Moreover, in invertebrates, dopamine (DA) acts as the major molecule used in neural systems. In vertebrates, l-norepinephrine (NEP) emerges as the major end of the catecholamines. The voltammetric behavior of 1 mmol L^{-1} MO and 1 mmol L^{-1} DA mixtures were investigated by DPV in B-R buffer pH 7.4 and scan rate 10 mV/s . As shown in Fig. (8A), MO and DA yielded two well-defined oxidation peaks at 163.08 mV and 349.56 mV with potential peak separation 186.48 mV at GNFMCPCE and higher current response than in case of unmodified CPE.

Morphine withdrawal increases the turnover of NPE in the heart so studying both compounds in presence of each other is necessary. The DPV technique (figure 8B) shows the voltammetric response of 1 mM MO solution containing 1 mM NEP in B-R buffer (pH 7.4). This figure illustrates that it is possible to discriminate MO from NEP with good separation in peak potential ($\Delta E = 195.16 \text{ mV}$) since they appear as one broad peak at bare CPE.

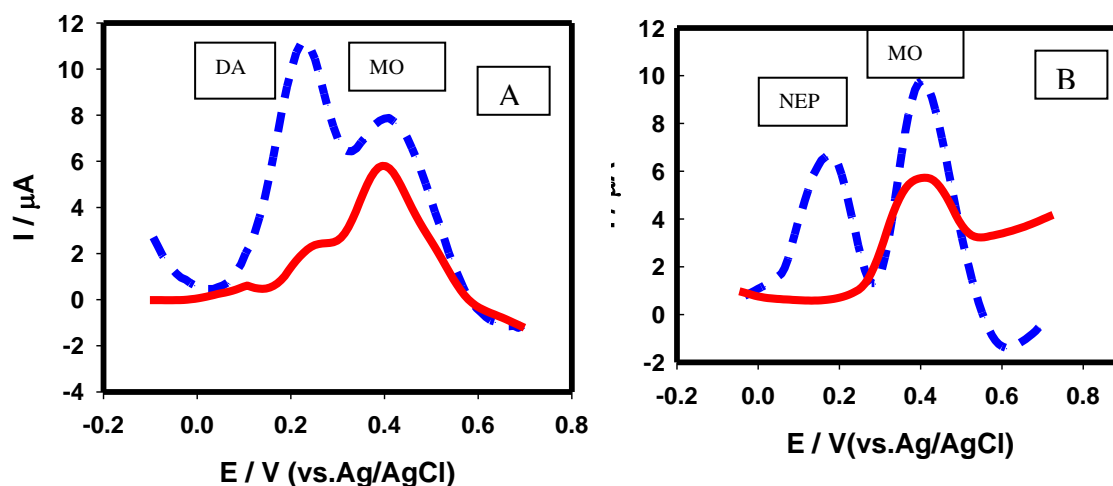


Figure 8. **A)** The differential pulse voltammograms of equimolar solution 1 mmol L^{-1} of both MO and DA in B-R buffer pH 7.4 and scan rate 10 mV/s at bare CPE (solid line) and GNFMCPCE (dashed line). **B)** The differential pulse voltammograms of equimolar solution 1 mmol L^{-1} of both MO and NEP in B-R buffer pH 7.4 and scan rate 10 mV/s at bare CPE (solid line) and GNFMCPCE (dashed line).

3.5. General procedure for the determination of MO in the pure form

Pulse voltammetric techniques, such as DPV, are effective and rapid electroanalytical techniques with well-established advantages, including good discrimination against background current and low detection limits. To prove the sensitivity of GNFMCPCE towards the electrochemical measurement of MO, the effect of changing the concentration of MO in B-R buffer pH 7.4, using DPV

mode was studied (Fig. 9) The following are the parameters for the DPV experiments: $E_i = 100$ mV, $E_f = +600$ mV, scan rate = $10 \text{ mV}\cdot\text{s}^{-1}$, pulse width = 25 ms, pulse period = 200 ms, and pulse amplitude = 10 mV.

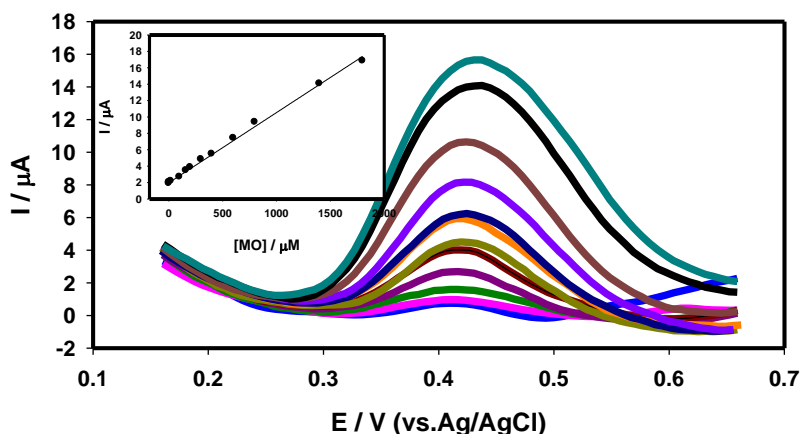


Figure 9. The effect of changing the concentration of MO, using DPV mode at GNFMCPE in 0.04M B-R buffer pH 7.4 and scan rate 10 mV/s. The inset: The calibration plot of the oxidation peak current versus the concentration range of MO.

Table 1. Comparison of several surfaces mentioned for the determination of morphine.

Electrode used	Detection limit	Reference
MIP modified electrode	0.2 mM	[12]
CoHCF	0.5 μM	[14]
Pretreated GCE	0.2 μM	[17]
PB/Pd-Al	0.8 μM	[21]
AuNpCPE	4.21 nM	[25]
GNFMCPE	3.51 nM	This work

The corresponding calibration plot was given in the inset of (Fig.9). The calibration plot was linearly related to MO concentration over the range of 1.0×10^{-6} to $18.0 \times 10^{-4} \text{ mol L}^{-1}$ with correlation coefficient of 0.9994. The limit of detection (LOD) and the limit of quantitation (LOQ) were calculated from the oxidation peak currents of the linear range using the following equations:

$$\text{LOD} = 3s/m$$

$$LOQ = 10s/m$$

Where s is the standard deviation of the oxidation peak current (three runs) and m is the slope ($\mu\text{A}\text{M}^{-1}$) of the related calibration curves, and they were found to be $3.507 \times 10^{-9} \text{ mol L}^{-1}$ and $1.169 \times 10^{-8} \text{ mol L}^{-1}$ respectively. Both LOD and LOQ values confirmed the sensitivity of GNFMCPPE.

Table 1 shows a comparison of several surfaces mentioned in literature for the determination of morphine. Our work showed the lowest limit of detection compared to the other values mentioned in the literature using other modified electrodes.

3.6. Electrochemical impedance spectroscopy (EIS) studies

EIS is an effective tool for studying the interface properties of surface-modified electrodes. EIS data were obtained for GNFMCPPE at ac frequency varying between 0.1Hz and 100 kHz. It is clear that the impedance responses of $\text{K}_4 \text{Fe}(\text{CN})_6$ show great difference between the three cases, i.e. in case of bare CP electrode, the impedance spectra of $\text{K}_4 \text{Fe}(\text{CN})_6$ includes a semicircle with larger diameter than in case of AuNpCPE and GNFMCPPE. The diameter of semicircle diminishes markedly and the charge transfer resistance of electrooxidation of $\text{K}_4 \text{Fe}(\text{CN})_6$ decreases greatly, and the charge transfer rate is enhanced in case of using GNFMCPPE.

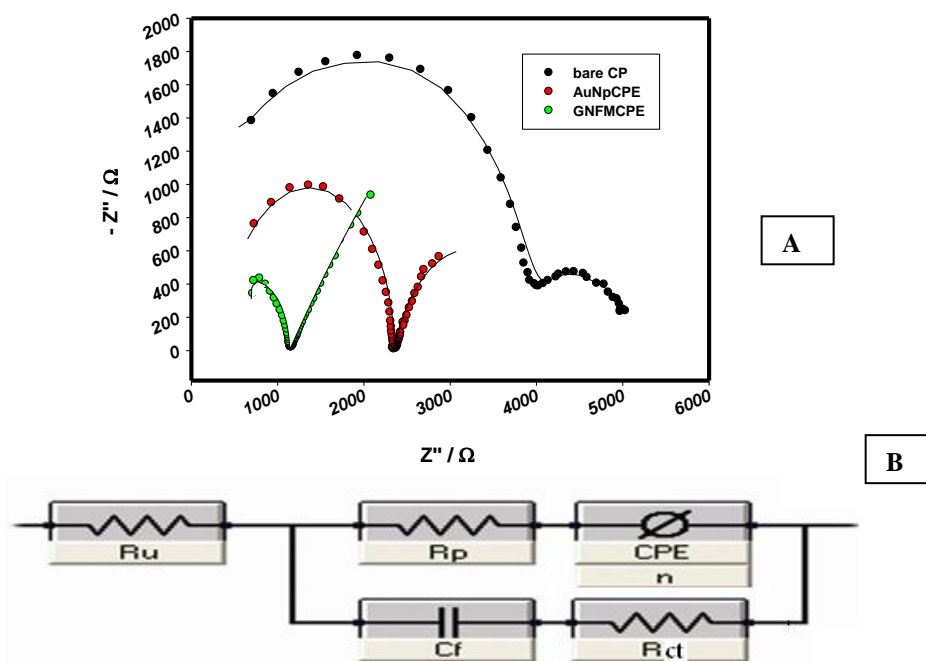


Figure 10. A) The typical impedance spectrum presented in the form of the Nyquist plot for CP-electrode (a) AuNpCP-electrode(b) and GNFMCPPE (c) against 5 mmol/L $\text{K}_4 \text{Fe}(\text{CN})_6$ at oxidation potential equivalent to 315, 300 and 280mv respectively. symbols and solid lines represent the experimental measurements and the computer fitting of impedance spectra, respectively). B) Equivalent circuit used in the fit procedure of the impedance spectra.

The experimental data were compared to an “equivalent circuit” (fig.10B). In this circuit, R_u is the solution resistance, its values depend on the solution and the distance between working electrode and reference electrode, R_p is the polarization resistance, CPE represents the predominant diffusion influence on the charge transfer process, n is its corresponding exponents. C_f is the capacitance of the double layer and R_{et} is the charge-transfer resistance associated with the oxidation of the drug. R_{et} of the electrode reaction is the only circuit element that has a simple physical meaning describing how fast the rate of charge transfer during electrocatalytic oxidation changes with the electrode potential or bulk concentration of drug in solution.

Table 2 lists the best fitting values calculated from the equivalent circuit for the impedance data at 280 mV, 300 and 315 mV for each electrode. The data validation, carried out proves that experimental results fit reasonably and are in a good agreement with the proposed circuit model. From the data indicated in Table 2, the value of solution resistance, R_u , was almost constant within the limits of the experimental errors. On the other hand, the ionic/electronic charge transfer resistance shows noticeable decrease in values in case of GNFMCPPE compared to AuNpCPE and bare CP electrode, which indicates less electronic resistance and more facilitation of charge transfer of GNFMCPPE > AuNpCPE > bare CP electrode. The capacitive component of the charge at GNFMCPPE is relatively higher compared to that at AuNpCPE and bare CP electrode. This is explained in terms of the increase in the ionic adsorption at the electrode/electrolyte interface. Moreover, the decrease in the interfacial electron transfer resistance is attributed to the selective interaction between gold nanoparticles and the analyte that resulted in the observed increase in the current signal for the electro-oxidation process.

Table 2. Electrochemical impedance spectroscopy fitting data corresponding to Fig 10(A and B).

Electrode	E/mV	R_p ($k\Omega\text{ cm}^2$)	R_u ($k\Omega\text{ cm}^2$)	C_f (μFcm^{-2})	R_{et} ($k\Omega^{-1}\text{ cm}^{-2}$)	CPE (μFcm^{-2})	n
Bare CPE	315	4.721	0.22	1.16	3.37	2.65	0.25
GNMCPE	300	3.570	0.34	1.36	0.87	7.35	0.59
modified	280	1.755	0.38	1.60	0.84	9.82	0.77

3.7. Validation method in urine

Successive additions of 10 μ l of 1mmol/L MO provided by the National Organization for Drug Control and Research of Egypt were added to 5 ml of stock solution containing (1:400 v/v) urine to B-R buffer (pH 7.4) was examined at scan rate 10 mV/s using DPV. The calibration curve (fig 11) gave a straight line in the linear dynamic range 2×10^{-6} mol L $^{-1}$ to 4×10^{-5} mol L $^{-1}$ with correlation coefficient, $r = 0.9994$, the LOD is 4.27×10^{-9} mol L $^{-1}$ and LOQ is 1.423×10^{-8} . Four different concentrations on the calibration curve are chosen to be repeated five times to evaluate the accuracy and precision of the proposed method which is represented in (table-3).

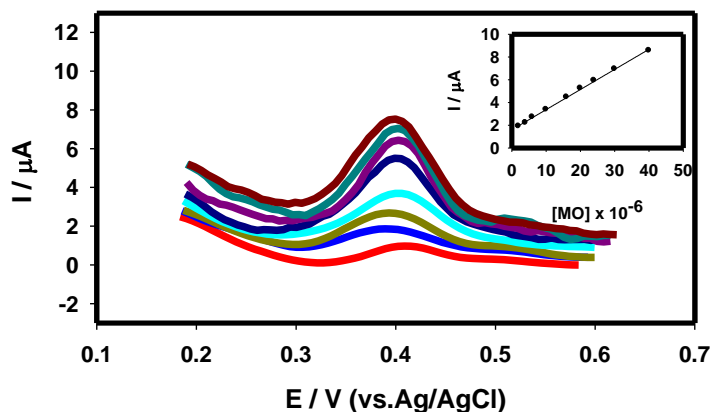


Figure 11. Validation of the quantitative assay of the MO in urine using B-R buffer pH 7.4, at scan rate 10 mV/s. The inset: the relation between MO concentration in urine and the current responses

Table 3. Evaluation of the accuracy and precision of the proposed method for the determination of (MO) in urine sample.

[MO]added (M) x 10 ⁻⁵	[MO] Found ^a (M) x 10 ⁻⁵	Recovery (%)	SD x 10 ⁻⁶	S.E ^b x 10 ⁻⁶	C.L. ^c x 10 ⁻⁶
5.0	5.018	100.30	0.47	0.19	0.37
10.0	9.990	99.900	0.35	0.15	0.46
12.0	12.04	100.30	0.41	0.20	0.65
18.0	18.04	100.20	0.42	0.21	0.68

4. CONCLUSION

In the present work, novel biosensor based on modification of CP-electrode with Ferrocene and gold nanoparticles was used for electrochemical determination of MO. The advantages of the gold nanoparticles / Ferrocene enhanced the sensitivity of the CP-electrode significantly. The experimental conditions such as number of cycles of Ferrocene deposition, pH, scan rate and types of electrolytes were optimized to find the highest sensitivity for the determination of MO. The results showed that the method was simple and sensitive enough for the determination of MO in clinical preparations (human urine) under physiological conditions with good precision, accuracy, selectivity and very low detection limit (nano-molar).

In this paper, we demonstrated the selective determination of MO in presence of AA and UA in 0.04 M B-R buffer (pH 7.4) using GNFMCPPE. The bare CP-electrode failed to resolve the voltammetric signals of a mixture of MO from AA and UA. On the other hand, the GNFMCPPE

enhanced the current signals of MO, while the oxidation peak current of AA disappeared and low response of UA obtained. Also a good binary separation of MO with DA and MO with NEP in 0.04 M B-R buffer (pH 7.4) using GNFMCPPE was achieved with good potential peak separation.

ACKNOWLEDGMENT

The authors would like to express their gratitude to the University of Cairo (Office of President for Graduate Studies and Research) for providing partial financial support through "The Young Researchers' Program." We would like to acknowledge the financial support by the National Organization for Drug Control and Research (NODCAR, Egypt).

References

1. J. Stjernsward, *Cancer Surv.* 7 (1988) 195.
2. H. M. Lee, C. W. Lee, *J. Anal. Toxicol.* 15(1991) 182.
3. G. Chari, A. Gulati, R. Bhat, I. R. Tebbett, *J. Chromatogr.* 571(1991) 263.
4. F. Tagliaro, D. Franchi, R. Dorizzi, M. Marigo, *J. Chromatogr.* 488(1989) 215.
5. M. E. Soares, V. Seabra, M. L. Bastos, *J. Liq. Chromatogr.* 15(1992) 1533.
6. G. Sakai, K. Ogata, T. Uda, N. Miura, N. Yamazoe, *Sens. Actuators B* 49 (1998) 5.
7. H.X.Hao, H. Zhou, J. Chang, J. Zhu, T. X. Wei, *Chin. Chem. Lett.*, 22, (2011) 477.
8. D.J. Chapman, S.P. Joel, G.W. Aherne, *J Pharmaceut. Biomed.*, 12 (1994) 353.
9. P.K. Owens, L. Karlsson, E.S.M. Lutz, L.I. Anderson, *Trend. Anal. Chem.*, 18 (1999) 146.
10. K. Haupt, K. Mosbach, *Chem. Rev.*, 100 (2000) 2495.
11. K. C. Ho, C. Y. Chen, H. C. Hsu, L. C. Chen, S.C. Shiesh, X. Z. Lin, *Biosens. Bioelectron.*, 20(2004) 3.
12. W.M. Yeh, K.C. Ho, *Anal. Chim. Acta*, 542(2005) 76.
13. A. M. Idris, A. O. Alnajjar, *Talanta*, 77(2008) 522.
14. F. Xu, M. N. Gao, L. Wang, T. S. Zhou, L. T. Jin, J. Y. Jin JY, *Talanta*, 58 (2002) 427.
15. K. C. Ho, C. Y. Chen, H. C. Hsu, L. C. Chen, S. C. Shiesh, X. Z. Lin, *Biosens. Bioelectron.*, 20(2004) 3.
16. C. H Weng, W. M. Yeh, K. C. Ho, G. B. Lee, *Sensor Actuators B*, 121(2007)576.
17. F. Li, J. X. Song, D. M. Gao, Q. X. Zhang, D. X. Han, L. Niu, *Talanta*, 79 (2009) 845.
18. N. F. Atta, A. Galal, R. A. Ahmed, *Electroanalysis*, 23 (2011) 737.
19. R.S. Schwartz, C.R. Benjamin, *Anal. Chim. Acta* 141 (1982) 365.
20. B. Proksa, L. Molnár, *Anal. Chim. Acta*, 97(1978)149.
21. H. M. Pournaghi-Azar, A. Saadatirad, *J. Electroanal. Chem.*, 624(2008)293.
22. A. Niazi, A. Yazdanipour, *Chin. Chem. Lett.*, 19 (2008) 465.
23. A. Niazi, J. Ghasemi, M. Zendehtdel, *Talanta*, 74 (2007) 247.
24. A. Salimi, R. Hallaj, G.R. Khayatian, *Electroanalysis*, 17 (2005) 873.
25. N. F. Atta, A. Galal, S. M. Azab, *J. Electrochem. Sci.*, 6 (2011) 5066.
26. N. F. Atta, A. Galal, E.H.El-Ads, *Electrochim. Acta*, 69 (2012) 102.
27. N. F. Atta, A. Galal, E.H.El-Ads, *Talanta*, 93 (2012) 264.
28. N. F. Atta, A. Galal, E.H.El-Ads, *Analyst*, 137 (2012) 2658.
29. S. Nakahama and R.W. Murray, *J. Electroanal. chem.*, 158 (1983) 303.
30. R.A. Saraceno, G.H. Riding, H.R. Allock and A.G. Ewing, *J. Am. Chem. Soc.*, 110 (1988) 980.
31. A. Mertz and A.J. Bard, *J. Am. Chem. Soc.*, 100 (1978) 3222.
32. A.L. Crumblis, D. Cooke, J. Castillo and P. Wisian-Neilson, *Inorg. Chem.*, 32 (1993) 6088.

33. C.M.Casado, I.Cuadrado, M.Moran, B.Alonso, F.Lobete and J.Losada, *Organometallics*, 14 (1995) 2618.
34. A.D.Ryabov, A.Amon, R.K.Gorbatova, E.S.Ryabova and B.B.Gnedenko, *J. Phys. Chem.*, 99 (1995) 14072.
35. C.L.Wang and A.Mulchandani, *Anal. Chem.*, 67(1995) 1109.
36. L.Fernandez and H.Carrero, *Electrochim. Acta*, 50 (2005) 1233.
37. J. B. Raoof, R. Ojani and M. Baghayer, *Chin. J. Catal.*, 32(2011) 1685.
38. J. B. Raoof, R. Ojani and M. Baghayer, *Sens. Actuators B*, 143 (2009)261.
39. A.Taherkhani, H.K-Maleh, A.A.Ensafi, H.Beitollahi, A.Hosseini, M.A.Khalilzadeh and H.Bagheri, *J. Chin. Chem.. letters*, 23 (2012) 237.
40. J. Zheng, X. Zhou, *Bioelectrochemistry*, 70 (2007) 408.
41. T.Skeika, C.R.Zuconelli, S.T.Fujwara and C.A.Pessoa, *Sensors*, 11(2011)1361.
42. A.Galal, N.F.Atta, S.A.Darwish and A.M.Abdallah, *Chem. Soc. Jpn*, 70(1997) 1769.
43. X. Jiang and X. Lin, *Anal. Chim. Acta*, 537 (2005) 145.
44. Samir D. Roy and Gordon L. Flynn, Solubility behavior of narcotic analgesics in aqueous media. *Pharmaceut. research*, 6 (1989) 2.
45. W. Qijin, Y. Nianjun, Z. Haili, Z. Xinpin, X. Bin, *Talanta*, 55 (2001) 459.
46. V.S. Vasantha, S.-M. Chen, *J. Electroanal. Chem.*, 592 (2006) 77.
47. L. Ahtee, L.M.J. Attila, K.R. Carlson, H. Haikala, *Pharmacol. Exp. Ther.* 249 (1989) 303.
48. G.D. Chiara, A. Imperato, *J. Pharmacol. Exp. Ther.* 244 (1988) 1067.
49. G.K. Aghajanian, J.H. Kogan, B. Moghaddam, *Brain Res.* 6336 (1994) 126.
50. E. Acquas, G.D. Chiara, *J. Neurochem.* 58 (1992) 1620.
51. G.V. Rebec, C.P. Pierce, *Prog. Neurobiol.* 43 (1994) 537.
52. L.D. Angeli, *Brain Res.* 670 (1995) 303.
53. G. Paxinos, C. Watson, *Academic Press, New York*, 1982.
54. V.A. Roginsky, T.K. Barsukova, G. Bruchelt, H.B. Stegmann, *Pharmacol. Res.*31 (1995) 141.